Development of confined concrete models and applications in capacity prediction of concrete-filled box-shaped steel columns

K. A. S. Susantha*, Hanbin Ge**, Tsutomu Usami***

*JSPS Research Fellow, D.Eng., Dept. of Civil Engineering, Aichi Institute of Technology
(Yachigusa 1247, Yagusa-cho, Toyota-shi, 〒470-0392)
**Assoc. Professor, D.Eng., Dept. of Civil Engineering, Nagoya University
(Furo-cho, Chikusa-ku, Nagoya-shi, 〒464-8603)
***Professor, D.Sc., D.Eng., Dept. of Civil Engineering, Nagoya University
(Furo-cho, Chikusa-ku, Nagoya-shi, 〒464-8603)

This paper presents a recently developed confined concrete model and an analytical method that uses the specific features of this model to predict the capacity of partially concrete-filled box-shaped steel bridge piers subjected to strong ground motions. The proposed capacity prediction method includes the well-known fiber analysis technique together with a newly introduced failure criterion that helps to detect the ultimate point. In this failure criterion, occurrences of failures in steel and concrete at composite parts are considered in addition to the steel failure at the hollow part of columns. Test specimens of both relatively thick- and thin-walled sections were analyzed and numerical results of predicted ductility and ultimate strengths were compared with those of the experimental results. The predictions were also made by means of the previously available procedures that use simple concrete stress-strain relations. It was revealed from the comparisons that the ductility is more sensitive to the prediction method than the ultimate strength. The proposed method was found to give safe and better predictions in most of the cases.
Key Words : Concrete-filled steel column, Fiber analysis, Strength, Stress-strain relation, Ultimate state.

1. INTRODUCTION

The excellent earthquake resisting characteristics of concrete-filled steel columns have resulted in many experimental and analytical investigations to examine the behavior of concrete-filled steel bridge piers. Numerous such studies have also been largely emerged after the extensive structural damages of steel bridge piers caused by the 1995 Hyogoken-Nanbu Great Earthquake in Japan. It is evident that the most of the structural failures have occurred due to the severe local and overall interaction buckling of steel plates. By concrete infilling, such failures can be prevented or delayed considerably.

At present several experiments on the behavior of concrete-filled steel columns can be found in the literature (e.g., Ge and Usami[1), 2)], Joint Research Report[3)]). The high cost and various other difficulties confronting in conducting such experimental work limit the scope of the study. Hence, numerical methods become an essential means of avoiding such difficulties. As a result, in recent years, a great number of analytical investigations have been carried out to examine the behavior of concrete-filled steel columns (e.g., Tang et al.[4)], Watanabe et al.[5)], Schneider[6)], Ge et al.[7)]). One of the simplest yet powerful technique used in predicting the load-displacement behavior of concrete-filled columns is fiber analysis. This analysis method involves with uniaxial constitutive relations of concrete and steel. At present, an accurate stress-strain relationship for steel is available for application in fiber analysis[8)]. However, only a few models can be found in the case of filled-in concrete[4), 5), 9)]. These models are either simple or do not include all the affecting factors such as width-to-thickness ratios of sections, concrete and steel strengths, shape of the sections, etc. Therefore, it is important to establish a generalized stress-strain relationship having a wider range in its application.

This paper includes an attempt made to fulfill the need of complete stress-strain relationship and its application in the fiber analysis for ultimate state prediction of concrete-filled steel bridge piers. To this end, a summary of recently proposed uniaxial concrete model is presented. An analytical method, which is based on the fiber analysis technique and a new failure criterion, is subsequently described. Finally, numerical results of several test specimens are illustrated to explore the effectiveness of proposed method.

2. STRESS-STRAIN MODELS

A brief explanation of recently proposed uniaxial stress-strain model for filled-in concrete and a summary of previously available simple stress-strain models, which are later used in comparison purposes, are presented in this section. The proposed model has its application in both unstiffened and stiffened section steel columns. The section also includes the type of steel model employed in the proposed analysis.

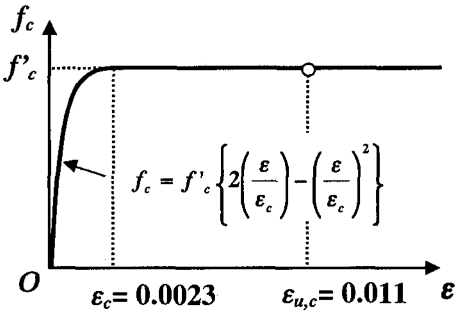

(a) Previous (1996)

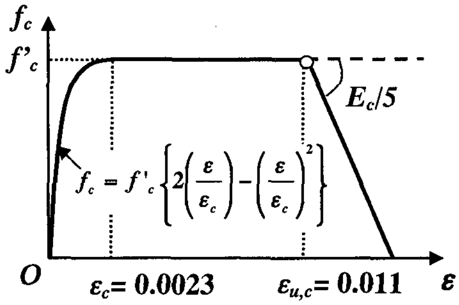

(b) Previous (2001)

Fig. 1 Previous concrete stress-strain models

2.1 Previous Concrete Stress-Strain Models

Two types of models found in the work by Usami[10] and Ge et al.[7] are shown in Figs. 1(a) and 1(b), respectively. In these models, the increase of strength due to the confinement effects is simply treated by taking the uniaxial compressive strength as its confined strength. In both models, failure strain of concrete has been defined as 0.011 regardless of the geometry and material properties of the columns. The model "previous 1996" does not include any softening behavior beyond the peak, whereas, the "previous 2001" model has a sudden strength drop beginning at the strain level of 0.011 given by a straight line having a falling branch slope of $E_c/5$.

2.2. New Stress-Strain Model for Filled-in Concrete

Two models, one for relatively thick-walled section columns, and the other for relatively thin-walled section columns, as shown in Figs. 2(a) and 2(b), are proposed. The relatively thick-walled section is defined as when the value of width-to-thickness ratio parameter ($R = R_w$ or R_f) is less than or equal to 0.85. Otherwise, a section is defined as relatively thin-walled. This limit is taken based on the buckling strength formula proposed by Ge et al.[11] for the component plates. The parameter R is given by

$$R = \frac{b}{nt}\sqrt{\frac{12(1-\upsilon^2)}{4\pi^2}}\sqrt{\frac{f_y}{E_s}} \tag{1}$$

where b is the flange (or web) plate breadth, E_s and υ are respectively the Young's modulus and the Poison's

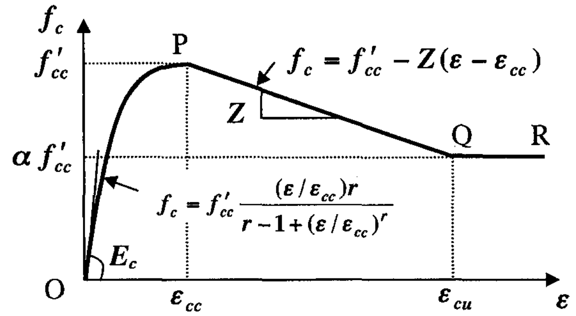

(a) for relatively thick-walled box section

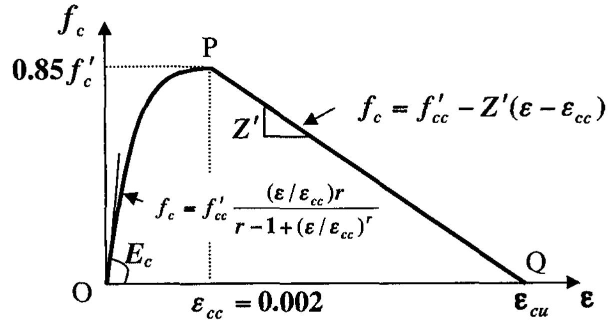

(b) for relatively thin-walled box section

Fig. 2 Proposed concrete stress-strain models

ratio of steel, n is the number of subpanels created by the stiffeners (=1.0 for unstiffened plates).

(1) Model for thick-walled section columns

In the case of model for application in thick-walled section columns, the stress-strain curve up to the peak point is expressed by Eq. (2), which was originally suggested by Mander et al.[12] for concrete confined by means of lateral ties or stirrups. That is,

$$f_c = f'_{cc}\frac{(\varepsilon/\varepsilon_{cc})r}{r-1+(\varepsilon/\varepsilon_{cc})^r} \tag{2}$$

where

$$r = \frac{E_c}{(E_c - f'_{cc}/\varepsilon_{cc})} \tag{3}$$

$$\varepsilon_{cc} = \varepsilon_c\left[1+5\left(f'_{cc}/f'_c - 1\right)\right] \tag{4}$$

Notations f_c and ε denote the longitudinal compressive stress and strain, respectively, and E_c stands for the tangent modulus of elasticity of concrete. The strain at unconfined concrete strength, ε_c, is taken to be 0.002. In the case of relatively thick-walled sections, the confined concrete strength, f'_{cc}, is given by

$$f'_{cc} = 0.85f'_c + 4.0f^*_{rp} \tag{5}$$

with

$$f^*_{rp} = -6.5R\frac{f'^{1.46}_c}{f_y} + 0.12f'^{1.03}_c \tag{6}$$

where f'_c and f_y (in MPa) stand for the unconfined concrete strength and the yield stress of steel, respectively. Term f^*_{rp} is the maximum average lateral pressure on concrete which has been proposed by means of an extensive parametric analysis of a concrete-steel interaction model as described in Susantha *et al.*[13].

The descending branch up to the ultimate strain, ε_{cu}, is given by

$$f_c = f'_{cc} - Z(\varepsilon - \varepsilon_{cc}) \tag{7}$$

where

$$Z = 23400R \cdot (f'_c / f_y) - 91.26 \geq 0 \tag{8}$$

$$\varepsilon_{cu} = 14.5[R \cdot (f'_c / f_y)]^2 - 2.4R \cdot (f'_c / f_y) + 0.116, \quad (0.018 \leq \varepsilon_{cu} \leq 0.04) \tag{9}$$

Certain calibration procedure has been carried out to propose expressions for the parameters Z (in MPa) and ε_{cu} based on the available experimental results, as described in Susantha *et al.*[13]. A constant strength of $\alpha f'_{cc}$ is maintained beyond the limit ε_{cu}. The parameter α appearing in Fig. 2(a) is given by

$$\alpha = \left(1 - Z(\varepsilon_{cu} - \varepsilon_{cc}) / f'_{cc}\right) \geq 1.0 \tag{10}$$

(2) Model for thin-walled section columns

For sections with R greater than 0.85 (i.e., relatively thin-walled section columns), it is assumed that lateral pressure does not contribute for the strength enhancement of concrete, thus in such cases the value of f'_{cc} is eventually be given by $0.85f'_c$ according to Eq. (5). The limiting value of R (i.e., 0.85) is substituted in Eq. (8) to approximate the falling branch slope Z', which is then given by

$$Z' = 19800(f'_c / f_y) - 91.26 \geq 0 \tag{11}$$

No residual stress is assumed to be present at higher strain levels, thus, the stress at the strain level of ε_{cu} becomes zero, as shown in Fig. 2(b).

(3) Modification for stiffened section columns

In order to treat the concrete in stiffened steel box sections, a simplified approached is adopted. The key point for this simplification is to choose an appropriate value for R denoted by R_{eq} (*equivalent width-to-thickness ratio parameter*) to be used in the originally proposed expressions of f^*_{rp}, Z and ε_{cu}. This is done by taking into account the effects of stiffeners on the improvement of lateral pressure exerted on concrete core and, hence strength enhancement. This effect is dependent on the flexural rigidity of stiffeners. It is thought that the stiffener's slenderness ratio parameter, $\bar{\lambda}_s$, as defined in Usami and Ge[8] will be suited well to represent the stiffeners' effects on concrete behavior. It has also been found that the occurrence of local buckling can be neglected when $\bar{\lambda}_s$ is smaller than 0.20 in Usami[10]. Consequently, two extreme cases for R_{eq} are suggested based on the value of $\bar{\lambda}_s$ as follows:

$$R_{eq} = \begin{cases} R_f \cdot n & \text{for } \bar{\lambda}_s \geq 1.50 \\ R_f & \text{for } \bar{\lambda}_s \leq 0.1 \end{cases} \tag{12}$$

The lower limit of $\bar{\lambda}_s$ is selected as 0.15 instead of 0.20 for the sake of safety while upper limit of 1.50 can be considered as the case where the effects of stiffeners are negligible with respect to the confinement available. For intermediate values between 0.15 and 1.50, a linear interpolation is utilized to determine the value of R_{eq}. The same definition as adopted in the unstiffened sections is used to define thin- and thick-wall sections, by using R_{eq} instead of R.

Moreover, in the case of unstiffned rectangular-shaped columns, the use of larger of R_f or R_w computed for flange or web plate is recommended to use in Eqs. (6), (8) and (9). In the case of stiffened sections, R_{eq} is calculated for both web and flange plates and larger value is substituted in the relevant equations.

2.3. Stress-Strain Model for Steel

An elasto-plastic stress relation with strain hardening region as shown in Fig. 3 is employed in the analysis of this study. The material parameters of this model are corresponding to the kind of steel types SS400, SM490 and SM570, as described in Usami and Ge[8].

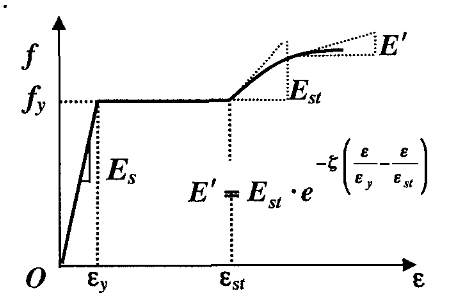

Fig. 3 Stress-strain diagram for steel

3. ANALYTICAL METHOD

3.1 Fiber Analysis

Fiber model analysis is usually considered as an effective and convenient way for capacity predictions of structures. This concept can be easily applied to the partially or fully concrete-filled steel columns in predicting the lateral load-lateral displacement characteristics. The important feature of this type of analysis is its simplicity and adequacy in practical design purposes. This concept is utilized in the present study. The analyses are conducted using a commercial general purpose finite element program, ABAQUS. Steel and concrete sections are discretized into number of fibers and uniaxial stress-strain relations of concrete and steel are assigned for corresponding fiber.

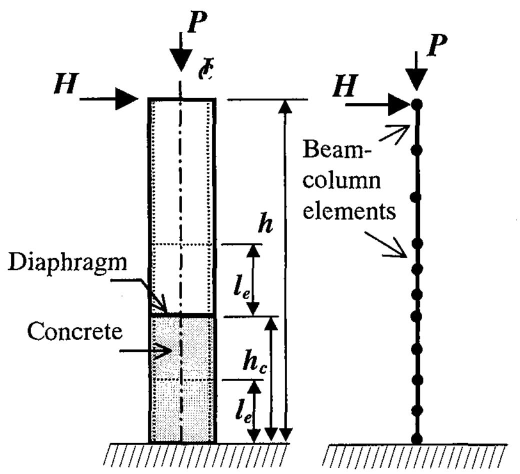

Fig. 4 Analytical model

As an example a finite element mesh adopted in the analysis is shown in Fig. 4. Here, failure of a column is examined through the average strain at two regions marked as l_e in the figure. At least two elements are recommended to be employed along the length l_e. It is usually understood that a highly refined element mesh is not necessary in ultimate state predictions using fiber analysis technique, nevertheless, relatively refined mesh should be assigned at the locations where failure is anticipated (i.e., at the vicinities of the base and above the top level of composite part). The effective failure length is adopted as the smaller of 0.7 times b (b is width of the section) and diaphragm spacing, l_d (Usami[10], Ge *et al.*[7]). Subsequently, a large deformation finite element analysis procedure is carried out for the columns subjected to monotonic lateral loads.

3.2 Failure Criterions

Generally, lateral load-lateral displacement relations obtained through fiber analysis do not exhibit a clear softening behavior. This is because the beam-column element cannot deals with the local buckling effects of steel plates and, also, uniaxial stress-strain relations of steel usually do not include any softening branch. In this circumstance, it is necessary to have a kind of failure criterion in order to determine the ultimate point.

(1) Previous method

In the previous studies, a failure criterion for the concrete-filled steel columns has been established based on the failure strain of steel and concrete. Here, the average strain of steel at hollow part and the average strain of concrete are compared with the failure strains of steel and concrete, respectively. The strains have been averaged at outer fibers of steel and concrete segments along the effective failure lengths. The earliest occurrence of either average strain equals to its failure strain has been defined as the ultimate point. Here, the concrete model, as shown in Fig. 1(a), is employed in the analysis. The steel failure strain has been taken by an empirical equation proposed by Usami *et al.*[14] based on the isolated plate analysis.

(2) Present method

Similar type of approach is adopted in this study by relating the column failure to the concrete failure strain and the steel failure strains at both the composite and hollow parts of the column. The failure strain of steel is adopted from the failure strain equations proposed by Zheng *et al.*[15] based on results of the stub-column analysis. They are given by Eqs. (13) and (14) for unstiffened and stiffened sections, respectively:

$$\frac{\varepsilon_{u,s}}{\varepsilon_y} = \frac{0.108\,(1-P/P_y)^{1.09}}{(R_f-0.2)^{3.26}} + 3.58(1-P/P_y)^{0.839} \le 20.0 \tag{13}$$

$$\frac{\varepsilon_{u,s}}{\varepsilon_y} = \frac{0.8\,(1-P/P_y)^{0.94}}{(R_f\bar{\lambda}_s^{\,0.18}-0.168)^{1.25}} + 2.78(1-P/P_y)^{0.68} \le 20.0 \tag{14}$$

The applicable ranges of R_f in Eqs. (13) and (14) are 0.2 ~ 0.8 and 0.2 ~ 0.7, respectively. Both equations are valid for P/P_y in the range of 0.0 to 0.5. Here, P_y is the squash load of the steel section.

The failure strain of concrete, $\varepsilon_{u,c}$, is defined as the strain when compressive stress has fallen to 80% of its maximum strength beyond the peak. The models shown in Fig. 2 are used in this method. It is clear that unlike the constant value adopted in the previous method, a more rational value, which represents the effects of geometrical and material properties of the columns, is utilized in the present procedure. Consequently, $\varepsilon_{u,c}$ can be expressed in terms of parameters f'_{cc}, ε_{cc} and Z (or Z') as follows:

$$\varepsilon_{u,c} = \varepsilon_{cc} + \frac{0.2f'_{cc}}{Z} \le 0.011 \tag{15}$$

The ultimate state of a column is recognized by comparing the displacements when damage indices D_{bc}, D_{bs} and D_s, which are defined as below, approach unity:

$$D_{bc} = \frac{\varepsilon_{a,bc}}{\varepsilon_{u,c}},\ D_{bs} = \frac{\varepsilon_{a,bs}}{\varepsilon_{u,s}},\ D_s = \frac{\varepsilon_{a,s}}{\varepsilon_{u,s}} \tag{16}$$

Here, $\varepsilon_{a,bc}$ and $\varepsilon_{a,bs}$ are respectively the average compressive strain of concrete and steel along the length l_e at composite part; $\varepsilon_{a,s}$ is the average compressive strain of steel along the length l_e above the composite part. All the average strains are computed at the outer fibers of relevant segments. Two kinds of comparisons have to be made in this procedure. First, the displacements corresponding to D_{bc}**=1.0** and D_{bs}**=1.0** are compared and the larger one is identified. Second, this displacement is compared with the displacement that corresponds to D_s**=1.0**. The lower of these two is defined as the ultimate displacement of the column. This failure criterion implies that if steel at the hollow part has not failed, the failure of the column is governed by the steel or concrete segment at composite part which fails at last. The ductility is defined as the ratio δ_u/δ_y, and the strength at this displacement level is taken as the ultimate strength, H_u/H_y.

As a summary, the major dissimilarities of the present and previous procedures can be listed as: (1) In present procedure, a new concrete stress-strain relation is adopted in which the effects of geometrical and material properties of columns on concrete behavior have been considered, whereas in the previous method, both factors have been neglected; (2) Concrete failure strain of present model is a function of key parameters such as R (i.e., R_f or R_w), $\bar{\lambda}_s$, f'_c and f_y while that of the previous model has a constant value irrespective of the tubes' properties; (3) As for the failure strain of steel, instead of equations proposed from the isolated plates, those based on the stub-column analysis are used in the present procedure; and (4) In the present procedure, the average strains of both the concrete and steel at the composite part are taken into account. In the previous method, only the average strain of concrete at the composite part is examined.

4. NUMERICAL RESULTS

Analytical results of 22 test specimens using the present and previous procedures are presented in this section together with their experimental results. Specimens are taken from the experimental series reported in Joint Research Report[3], Usami *et al.*[14], Usami[16], Amano *et al.*[17], and Saizuka and Usami [18]. All the specimens are categorized into thin- and thick-walled section columns depending on the value of R or R_{eq}. Accordingly, relevant stress-strain model of concrete is assigned for filled-in concrete. Subsequently, pushover analyses are carried out and

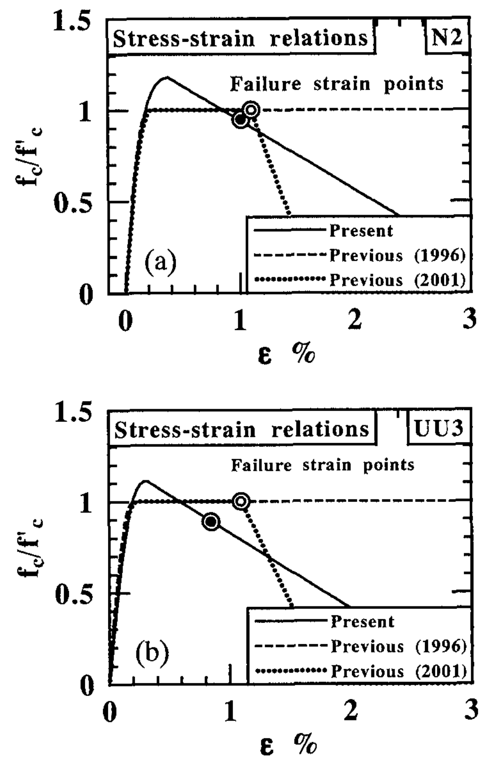

Fig. 6 Stress-strain relations under different concrete stress-strain models

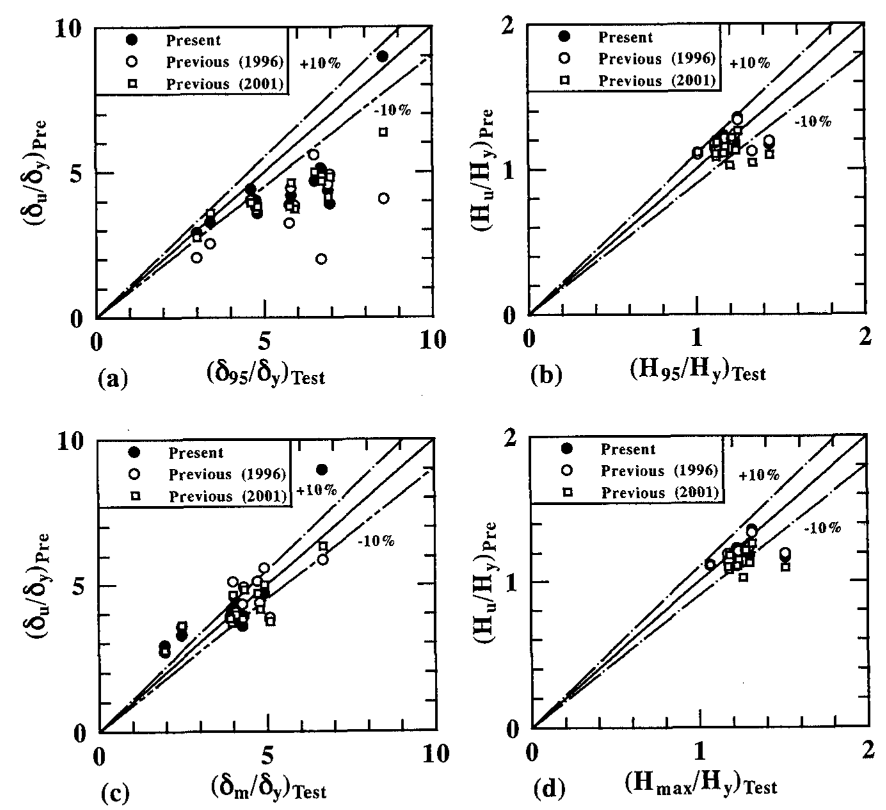

Fig. 5 Strength and ductility predictions of thick-walled section columns

lateral load-lateral displacement relations are obtained. The analyses are repeated using two types of previously available concrete models (i.e., models shown in Figs. 1(a) and 1(b)). Then, the ultimate point is determined using the above explained failure criterions. The identification of failure mode (i.e., failure at composite or hollow part) is also made for each method adopted. It has to be stated that the previous failure criterion is utilized with the results obtained using the model shown in Fig. 1(a) (Previous 1996). Meanwhile, the model shown in Fig. 1(b) (Previous 2001) involves with the new failure criterion.

According to Ge and Usami[2], the deformation capacity of test specimens can be defined as the state where the lateral load reaches the peak point (i.e., δ_m, H_{max}) or 95% of the peak load beyond the peak point (i.e., δ_{95}, H_{95}). In this study, the predicted strength and ductility capacities are compared with both of the indices above. It is noted that the envelopes of lateral load-lateral displacement hysteretic curves of test specimens are used in the comparisons.

4.1 Results of Thick-Walled Section Columns

A graphical illustration of strength and ductility predictions of specimens with thick-walled sections is shown in Fig. 5. First, comparisons are made with indices $(\delta_{95}/\delta_y)_{Test}$ and $(H_{95}/H_y)_{Test}$, as shown in Figs. 5(a) and 5(b). Second, similar types of comparisons are made with indices $(\delta_m/\delta_y)_{Test}$ and $(H_{max}/H_y)_{Test}$, as shown in Figs. 5(c) and 5(d). When comparisons are made using index $(\delta_{95}/\delta_y)_{Test}$, as seen in Fig. 5(a), the ductility predictions resulted from the present procedure seemed to be better than those of the previous (1996) method. However, only a slighter improvement can be visible when index $(\delta_m/\delta_y)_{Test}$ is concerned. The tendencies on the strength predictions through the present and the previous 1996 procedures are very similar when comparisons are made in terms of both $(H_{95}/H_y)_{Test}$ and $(H_{max}/H_y)_{Test}$, as illustrated in Figs. 5(b) and 5(d). However, in the case of the present and previous (2000) models (both models involved with the same failure criterion), the present model produced better predictions with respect to the strength. When ductility is concerned, both models were found to behave in a similar manner.

Two representative cases (i.e., specimens N2 and UU3, as shown in Fig. 6) are selected to discuss some aspects of the present and previous procedures with respect to the stress-strain relations and the failure strains of materials. It is noted that, although the values of parameter R_{eq} of these two columns are very much similar (i.e., 0.667 for N2 and 0.664 for UU3), the falling branch slopes of present model are different in these two examples (i.e., 862.1MPa for N2 and 2373.7MPa for UU3). This is mainly due to the effect of material strength ratio f'_c/f_y as explained in Eq. (8). Since the failure strain of concrete given by the present model depends on the falling branch slope, two

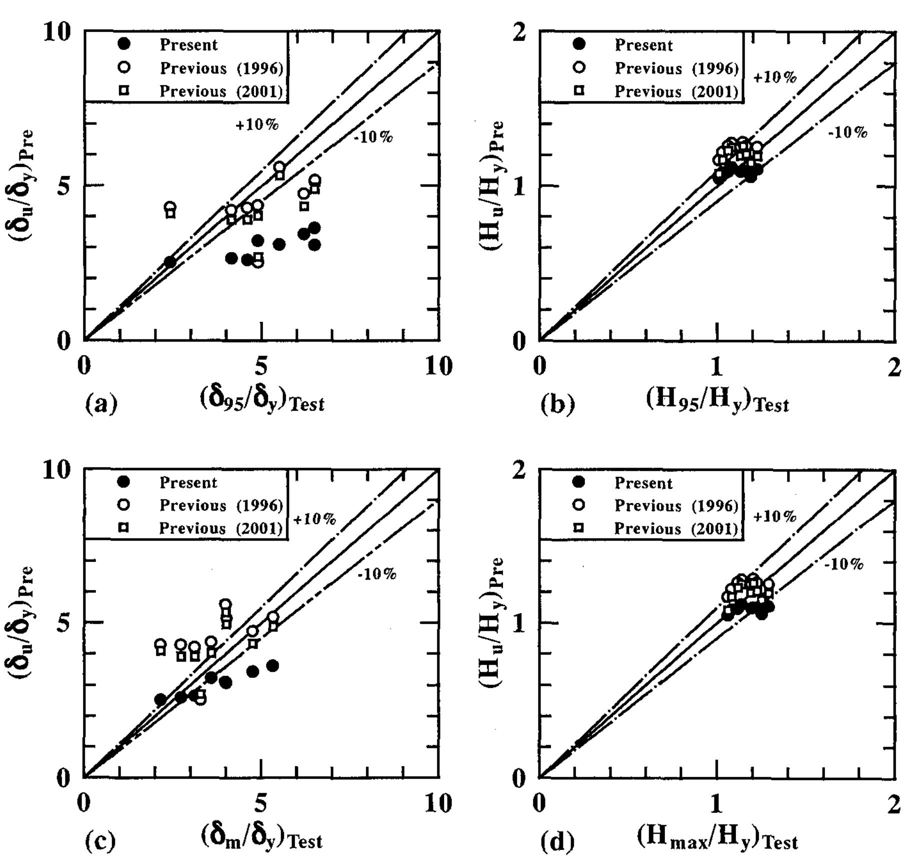

Fig. 7 Strength and ductility predictions of thin-walled section columns

different failure strain values can be observed in these two specimens (0.010 for N2 and 0.0085 for UU3). It is found that the predicted ductility of specimen N2 through present, previous 1996, and previous 2001 methods are 4.04, 3.81, and 3.69, respectively. The values of $(\delta_{95}/\delta_y)_{Test}$ and $(\delta_m/\delta_y)_{Test}$ are 4.75 and 3.96 respectively. The damage index D_{bc} governs the column failure when the previous 1996 model is used. In other two models, D_{bs} was involved. Hence, since the values of failure strains of these three methods are very much close, the apparent difference between predictions is mainly due to the adopted failure criterion. On the other hand, in the case of specimen UU3, the failure strains of the present and previous methods are quite different. It was found that the failure was governed by the damage index D_{bc} in all the methods. Thus, it is obvious that the significant difference in the ductility predictions (i.e., present method: -3.92, previous 1996: -4.92, and previous 2001: -4.83) is due to the different failure strains of concrete. The values of $(\delta_{95}/\delta_y)_{Test}$ and $(\delta_m/\delta_y)_{Test}$ of this specimen are 6.95 and 4.33, respectively.

4.2. Results of Thin-Walled Section Columns

Similar comparisons of predicted and experimental ductility and strength values of thin-walled section columns are illustrated in Fig. 7. According to Fig. 7(a), it is evident that the ductility predictions from present procedure are somewhat conservative when index $(\delta_{95}/\delta_y)_{Test}$ is concerned. In this case, quite good predictions could be obtained from the previous methods. However, it is clear from Fig. 7(c) that the present procedure is much better than the previous one when comparisons are made with parameter $(\delta_m/\delta_y)_{Test}$. Meanwhile, it is found that the strength predictions from present procedure shows good agreement with both of the strength indices, $(H_{95}/H_y)_{Test}$ and $(H_{max}/H_y)_{Test}$.

A representative case for stress-strain behavior of concrete in thin-walled section column given by the three types of concrete models is shown in Fig. 8. The failure points predicted by the present, previous 1996 and previous 2001 models are 3.10, 5.60 and 5.34, respectively. It was found that the failure strain of concrete given by present model (i.e., 0.005) did not govern the failure point. Here, the failure point was governed by the steel failure at the composite part. However, in other two models, concrete failure has contributed to the column failure. Therefore, the apparent difference between predicted failure points is mainly due to the effect of stress-strain behavior given by each model. Hence, the shift of damage index that governs the failure mode is dependent on the total stress-strain relation adopted. This means that making direct comparison of the effect of failure strains is meaningless if different damaged indices are involved in predicting the failure point.

In addition, it should be stated that, in both kinds of sections, the failure mode predicted through the present model matched with that of the observed modes except for very few cases. Finally, the above discussion revealed that the degree of effectiveness of the present method largely depends on the types of comparison made and the category to which a particular column belongs (i.e., thick- or thin-walled section). Nevertheless, in all the cases, the present method is found to be either better or conservative than the other methods discussed.

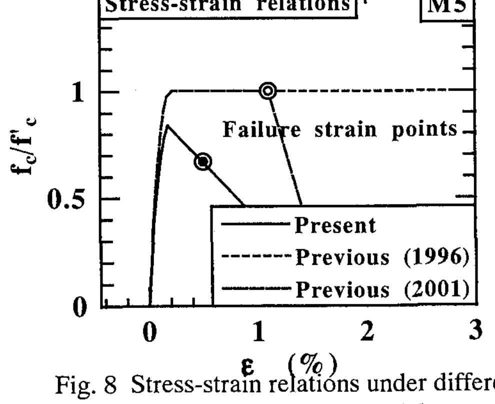

Fig. 8 Stress-strain relations under different concrete stress-strain models

5. CONCLUSIONS

Pushover analyses have been conducted using fiber analysis technique for the ultimate state prediction of partially concrete-filled steel columns. Both square- and rectangular-shaped columns with or without longitudinal stiffeners were considered. Using the comparisons of capacity predictions between the analysis and test, following conclusions are drawn as the main finding of this study:

(1) Pushover analysis with the help of fiber elements can effectively be carried out to predict the ultimate state of partially concrete-filled steel columns using the present analytical procedure.
(2) The prediction of the failure mode (i.e., failure at composite or hollow part) can be easily made using the proposed failure criterion. Also, in the event of failure at composite part, it can be checked which material governs the failure.
(3) The predictions using the present procedure are always on the safe side. The ductility predictions of thin-walled section columns are generally somewhat conservative, especially when ductility index $(\delta_{95}/\delta_y)_{Test}$ is concerned. However, it can be accepted in the light of practical design purposes.
(4) The present procedure is better than that of the previous (1996) method when ductility predictions of thick-walled section columns are concerned. The strength predictions of such columns are almost the same in both procedures.
(5) The introduction of confinement effects on strength enhancement and treatment of post peak strength deterioration of concrete are important.
(6) In relatively thin-walled section columns, the predictions by the present procedure are much better than those of previous method in terms of ductility. Both methods can be considered adequate in terms of strength predictions.

REFERENCES

1) Ge, H. B. and Usami, T.: Strength of concrete-filled thin-walled steel box columns :Experiment, J. Struct. Engrg., ASCE 118(11), pp.3036-3054, 1992.
2) Ge, H. B. and Usami, T.: Cyclic tests of concrete-filled steel box columns, J. Struct. Engrg., ASCE 122(10), pp.1169-1177, 1996.
3) Joint Research Report on Limit State Seismic Design of Highway Bridge Piers: Public Work Research Institute, Metropolitan Expressway Public Corporation, Hanshin Expressway Public Corporation, Nagoya Expressway Public Corporation, Kozai Club and Japan Association of Steel Bridge Construction, 1999 (in Japanese).
4) Tang, J., Hino, S., Kuroda, I. and Ohta, T.: Modeling of stress-strain relationships for steel and concrete in concrete filled circular steel tubular columns, Steel Construction Engineering, JSSC, 3(11), pp.35-46, 1996 (in Japanese).
5) Watanabe, H., Sakimoto, T., Senba, K. and Onishi, S.: A simplified analysis for the ultimate strength and behavior of concrete-filled steel tubular structures, Proc. of the Fifth International Colloquium on Stability and Ductility of Steel Structures, Japan, pp. 893-900, 1997.
6) Schneider, S. P.: Axially loaded concrete-filled steel tubes, J. Struct. Engrg., ASCE, 124(10), pp.1125-1138, 1998.
7) Ge, H. B., Asada, H., Susantha, K. A. S. and Usami, T.: Unified earthquake resistance verification procedure for partially concrete-filled steel piers with thin- and thick-walled sections, J. Struct. Engrg., JSCE, 47A, pp.783-792, 2001 (in Japanese).
8) Usami, T. and Ge, H. B.: Cyclic behavior of thin-walled steel structures-numerical analysis, Thin Walled Structures, 32(1/3), pp.41-80, 1998.
9) Tomii, M. and Sakino, K.: Experimental studies on the ultimate moment of concrete filled square steel tubular beam-columns. Transaction of Architectural Institute of Japan, No. 275, pp.55-63, 1979.
10) Usami, T. ed.: Interim guidelines and new technologies for seismic design of steel structures. Committee on New Technology for Steel Structures (CNTSS), JSCE, 1996 (in Japanese).
11) Ge, H. B. and Usami, T.: Strength analysis of concrete filled thin-walled steel box columns, J. Construct. Steel Res. 30, pp.259-281, 1994.
12) Mander, J. B., Priestly, M. J. N. and Park, R.: Theoretical stress-strain model for confined concrete, J. Struct. Engrg., ASCE 114(8), pp.1804-1826, 1988.
13) Susantha, K. A. S., Ge, H. B. and Usami, T.: Uniaxial stress-strain relationship of concrete confined by various shaped steel tubes, Engrg. Struct. 23(10), pp.1331-1347, 2001.
14) Usami, T., Suzuki, M., Mamaghani, I. H. P. and Ge, H. B.: A proposal for check of ultimate earthquake resistance of partially concrete-filled steel bridge piers, Struct. Mech/Earthquake Engrg, JSCE, 525(I-33), pp.69-82, 1995 (in Japanese).
15) Zheng, Y., Usami, T. and Ge, H. B.: "Ductility evaluation procedure for thin-walled steel structures, J. Struct. Engrg., ASCE, 126(11), pp.1312-1319, 2000.
16) Usami, T.: A seismic design method for steel piers through the pushover analysis, Proc. of the First Symposium on Ductility Design Method for Bridges, Tokyo, Japan, pp.183-186, 1998 (in Japanese).
17) Amano, M., Kasai, A., Usami, T., Ge, H. B., Okamoto, O. and Maeno, H.: Experimental and analytical study on elasto-plastic behavior of partially concrete-filled steel bridge piers, Struct. Engrg. JSCE Vol. 44A, pp.179-187, 1998 (in Japanese).
18) Saizuka, K. and Usami, T.: Verification of proposed method for checking the ultimate earthquake resistance of concrete filled bridge piers based on the hybrid test results, Struct. Mech/Earthquacke Engrg., JSCE No. 570/I-40, pp.287-296, 1997 (in Japanese).

（2001 年 12 月 7 日受付）

充填コンクリートの構成則の開発とコンクリート部分鋼製橋脚耐震解析への応用

K.A.S. Susantha, 葛 漢彬, 宇佐美 勉

本報告では箱形断面鋼部材に充填される拘束コンクリートの構成則を適用した，コンクリート部分充填鋼製橋脚の Capacity の耐震解析法について述べている．提案したコンクリート構成則と破壊基準による解析結果を，過去に提案されているコンクリート構成則と破壊基準による評価および実験結果と比較し，本手法が強度と変形能の評価を実験結果に比べて精度良く推定できることから，その有用性が示されている．